Topics in Catalysis (2021) 64:945–954
https://doi.org/10.1007/s11244-021-01434-z

ORIGINAL PAPER

Restructuring Effects in the Platinum-Catalysed Enantioselective Hydrogenation of Ethyl Pyruvate

G. A. Attard[1,2] · A. M. S. Alabdulrahman[1] · D. J. Jenkins[1] · P. Johnston[3] · K. G. Griffin[3] · P. B. Wells[1]

Accepted: 27 March 2021 / Published online: 18 June 2021

Abstract

The relative performance of Pt{111} and Pt{100} terraces in the enantioselective hydrogenation of ethyl pyruvate over cinchonidine-modified Pt/graphite has been investigated. Three series of 5% Pt/graphite catalysts have been prepared by sintering as-received material at temperatures in the range 400–1000 K. All underwent Pt particle growth and faceting as shown by transmission electron microscopy. Cyclic voltammetry has revealed the presence of {111}-terraces, {100}-terraces and related stepped features on these Pt surfaces. The performance of these surface structures as catalysts in the enantioselective hydrogenation of ethyl pyruvate to ethyl lactate has been determined using cinchonidine as the chiral modifier. As reported previously, the as-received catalyst provided an enantiomeric excess of ~ 40%(*R*). Two series of Pt/graphite catalysts having different particle size distributions were prepared by sintering in 5% H_2/Ar and one by sintering in pure Ar. Those sintered in H_2/Ar showed progressive Pt particle growth with faceting and considerable surface restructuring, whereas that sintered in Ar showed particle growth with little or no faceting and restructuring. The enantiomeric excess provided by the two series sintered in H_2/Ar showed a maximum of ~ 60%(*R*) [i.e. 80%(*R*)-lactate, 20%(*S*)-lactate] for catalysts sintered at 700 K, and this correlated with the fraction of Pt{111}-terraces in the surface which showed a coincident maximum. By contrast, the series sintered in pure Ar showed no such maxima, indicating the importance of restructuring in H_2 during catalyst preparation. Two catalysts sintered in H_2/Ar at 450 and 500 K showed unexpectedly low values of the enantiomeric excess and contained atypically high surface exposures of {100}-terraces, indicating that {100}-surfaces are deleterious to high catalyst performance. Poisoning of these {100}-surfaces by the selective adsorption of sulfur restored the enantioselectivity to its expected value. The two series of catalysts sintered in H_2/Ar gave comparable catalytic performance, but the one composed of smaller Pt particles contained a higher fraction of surface Pt{111}-terraces than the other, leading to an expectation of higher enantioselectivity. This suggested that some of the Pt{111}-surfaces identified by cyclic voltammetry are too small to accommodate the adsorption of the 1:1 modifier-reactant complexes necessary for rate-enhanced enantioselection, and hence do not contribute significantly to the overall reaction. Future catalyst design should therefore concentrate on preparation procedures that maximise {111}-terrace formation or contain poisons that deactivate {100}-surfaces.

Keywords Orito reaction · Enantioselective hydrogenation · Surface structure

1 Introduction

Enantioselective hydrogenation of α-ketoesters catalysed by supported platinum catalysts has attracted much attention since Orito and co-workers reported in 1978 that pre-adsorption of cinchona alkaloids onto conventional supported Pt catalysts rendered them enantioselective for methyl pyruvate hydrogenation [1, 2]. In this formally simple saturation of an activated carbonyl group, the chiral modifier cinchonidine induces preferential formation of R-lactate whereas cinchonine provides preferential S-lactate formation. Subsequent elaboration of the reactant, the alkaloid modifier, the

✉ G. A. Attard
attard@liverpool.ac.uk

✉ P. B. Wells
pbandmwells@che595.plus.com

[1] School of Chemistry, Cardiff University, Main Building, Park Pl, Cardiff CF10 3AT, UK

[2] Present Address: The Oliver Lodge Laboratory, Department of Physics, University of Liverpool, Liverpool L69 7ZE, UK

[3] Johnson Matthey, Orchard Road, Royston, Herts SG8 5HE, UK

solvent, the catalytic metal and its support, provided values of the enantiomeric excess (ee) ranging from 20 to 95% [3]. ($ee/\% = \{[R]-[S]\}10^2/\{[R]+[S]\}$).

Cinchona alkaloids possess a quinolone moiety by which they are adsorbed to the platinum surface [4–6] and a quinuclidine moiety, the N-atom of which plays a key role in the modifier/reactant interaction (if it is quaternised, enantioselectivity is lost [7]). These two ring systems are connected by a single chiral carbon atom, –CH(OH)–, which has the *R*-configuration in cinchonidine and the *S*-configuration in cinchonine. NMR spectroscopy [8, 9] and molecular modelling [10] have shown that cinchonidine possesses three low energy conformations, only one of which, the so-called open (3), has the quinuclidine-N atom directed away from the quinoline ring and suitably directed to form a 1:1-interaction with adsorbed α-ketoester [10, 11]. The relative proportions of these conformations change with the dielectric constant of the medium, open (3) being favoured in solvents of low dielectric constant [10, 11].

The site requirement for the adjacent co-adsorption of modifier and reactant is considerable. Reaction has been envisaged as taking place on extended {100}- and {111}-terraces, where molecular models suggest that about 25 coplanar Pt atoms are required [3, 12]. However, the most selective catalysts have been Pt on high-area oxide supports where the mean Pt particle size is small. For example, the 6.3% Pt/silica catalyst (EUROPT-1) has a well-documented mean particle size of 2 nm and gives ee = 75% [13]. Pt particles of this size probably have structures that approximate to the cubo-octahedral model, in which case the reactive surface consists of low index planes with many atoms situated at edges. The question then arises as to whether the reaction is structure sensitive to the point where these different site environments provide unique selectivities. If this were so, then the observed enantiomeric excess would be a mean value, and performance could be improved by selective poisoning of the least selective elements of the surface, or by preparation of metal particles having specific optimised surface structures.

To test this hypothesis, the present authors have used cyclic voltammetry to investigate selectivities at various step and terrace features at Pt catalyst surfaces. The technique requires conducting samples, and Pt/graphite has been the natural choice [14, 15]. Such catalysts provide only modest values of the enantiomeric excess (~ 50%) but this is advantageous if the various surface features are providing different enantioselectivities. Cyclic voltammograms (CVs) of Pt/graphite show features at 0.06, 0.20, 0.28, and 0.47 V (versus a Pd/H reference electrode) assigned (by comparison with single crystal data) to the presence of $\{111\}_{terr} \times \{111\}_{step}$ steps, $\{100\}_{terr} \times \{111\}_{step}$ steps, {100} terraces, and {111} terraces [16]. Adsorption of Bi onto Pt/graphite reduced enantiomeric excess, whereas adsorption of S had the opposite effect [16]. The CVs showed that Bi initially adsorbed at surface steps whereas S was preferentially adsorbed at {100}-terraces. Thus, sites adjacent to these steps were deduced to be relatively high selectivity sites whereas {100}-terraces were low selectivity sites, and performance was improved by their removal. Extensive adsorption of Bi left only {111}-terrace sites available for reaction, thus providing an estimate of the performance of this surface under these specific conditions [15]. 6.3% Pt/silica showed similar behaviour [15].

The relative proportions of step and terrace sites can be modified by sintering, i.e. by heating in a suitable atmosphere such as a flow of H_2 in Ar. Particle growth and faceting was accompanied by first an improvement and then a decline in enantioselectivity, the maximum performance (ee ~ 62%) being achieved for a sintering temperature of 700 K [16]. Such a particle size effect, for a range of Pt/carbon catalysts, was reported by Orito and co-workers in their early studies [1, 2].

The dependence of enantioselectivity on Pt particle shape became more evident when the behaviours of Pt nanoparticles of different shapes (predominantly cubic, octahedral, and cubo-octahedral) were compared [17]. Values of ee increased from 72 to 92% as the Pt{111}/Pt{100} ratio was increased. Theoretical studies indicated that cinchonidine was substantially more strongly adsorbed on Pt{100} terraces than on Pt{111}, and this was accompanied by the experimental observation that the alkaloid underwent more rapid partial hydrogenation on catalysts containing a higher proportion of Pt{100} surface. Thus, strategies for catalyst design should be directed towards either (i) enhancing the proportion of Pt{111} surface present, or (ii) minimising the proportion of Pt{100} surface or (iii) by introducing a selective poison to eliminate the contribution of Pt{100}.

There was an early report that a Pt colloid of mean particle size 1.4 nm stabilised by polyvinylpyrrolidone (PVP) and modified by cinchonidine provided an ee of 98%(R) in methyl pyruvate hydrogenation in ethanol [18]. A recent combined electrochemical-surface science study of PVP adsorption onto Pt single crystals has shown strong adsorption at step sites and at {100}-terraces but minimal adsorption at Pt{111}-terraces [19]. Moreover, in the presence of PVP, adsorption of Pt atoms onto Pt{hkl} showed marked preference for {100} facet formation on Pt{100} surfaces, but no analogous {111} facet formation on Pt{111}. Thus, at low concentrations, PVP exerts shape control over platinum particle growth, enabling the formation of cubic particles in preference to octahedral or cubo-octahedral particles [19]. Very recently, it has been demonstrated that cinchonidine-modified PVP-capped 1 wt% Pt/alumina can provide ee = 95% in methyl pyruvate hydrogenation—a substantial improvement brought about by the presence of the capping agent [20]. The origin of the improvement was proposed to

be the selective exposure of high coordination terrace sites in the active catalyst, with PVP adsorbed on and thus blocking low coordination defect sites.

The earlier use of Bi and the later use of PVP as agents for the blocking of low-coordination sites in the title reaction has led to an apparent contradiction in the interpretation of their effects. Both give rise to rate enhancements, but adsorption of Bi reduces enantioselectivity [15] whereas PVP affords a significant increase [20]. In the hydrogenation of three alkynes to the corresponding alkenes over various Pt catalysts, the selective blocking of low coordination sites by Bi and by PVP prevents, in each case, the formation of di-σ/π-alkene intermediates which contribute to (unwanted) alkane formation [21]. The contrasting behaviours of these blocking agents in pyruvate ester hydrogenation may therefore reflect the existence of electronic or structural factors that have not, so far, been recognised.

In the present study, we re-examine earlier work by our group in the light of these recent developments but utilising quantitative measurements of Pt{111} terrace site populations in particular to assess their role in the enantioselective hydrogenation of ethyl pyruvate.

2 Experimental

2.1 Platinum Catalysts

5% Pt/graphite was supplied by Johnson Matthey. Three series of sintered Pt catalysts were prepared. In each case ~ 2 g of as-received material was placed in a silica boat in a tube furnace and air expelled by a flow of 5% H_2/Ar (Series 1 and 3) or by pure Ar (Series 2). Temperature was then raised at 10 K min^{-1} to the required sintering temperature and maintained there for 3 h (Series 1 and 2) or 4 h (Series 3). Samples were then allowed to cool naturally to ambient temperature.

Series 1 The characterisation of these Pt catalysts has been described [14–16]; details are presented here for comparison purposes. Samples were sintered at 400, 500, 600, 700, 800, and 1000 K. More extensive TEM images (Series 1 and Series 2 catalysts) than those already reported for theses samples in references 14–16 are provided in the Supplementary Information file.

Series 2 These catalysts were prepared at the same time as Series 1, using the same Pt/graphite stock. They were sintered at the same temperatures.

Series 3 This series was prepared later from nominally the same 5% Pt/graphite stock. The procedure was the same as that for Series 1 (i.e. sintering in 5% H_2/Ar) except that the sintering temperatures of 450, 600, 700, 800, and 900 K were maintained for 4 h.

High resolution transmission electron microscopy (HRTEM) was used to determine platinum particle size distributions (PSDs). Samples were examined at the Johnson Matthey Technology Centre using a Philips FEI Technai-F20 microscope operated at 200 kV and giving a resolution of 0.15 nm. For each catalyst, Images of several randomly selected areas gave comparable PSDs, indicating that the platinum was evenly distributed and reproducibly dispersed. A selection of the instrumentally determined PSDs, including those shown in Table 1, were checked by manual measurements using the same micrographs and a calibrated eye-piece; good agreement was obtained.

A notable (but not novel) feature of the sintering process was the advent of faceting, especially of the larger Pt particles. An approximate evaluation of faceting was made by measuring the fraction of particles that showed two or more clear 120° angles. (No distinction was made between a particle with two such angles and a fully hexagonal particle). The extents of faceting quoted are intended only as a guide (figures rounded to the nearest 5%).

2.2 Sulfided Pt/Graphite

Sulfided catalysts were prepared from Series 3 Pt/graphite sintered at 500 K and 700 K. In each case, 0.35 g samples of sintered catalyst were placed in a 100 ml glass bubbler and a specific volume (1–4cm^3) of aqueous 1.5 mM Na_2S added. H_2 was passed through the slurry for 0.5 h followed by N_2 for a further 0.5 h. The sulphided catalyst so formed was filtered under vacuum, washed with 200 ml ultrapure water, and dried at ambient temperature.

Table 1 Pt particle size distributions for Pt/graphite catalysts sintered at 700 K

	Pt particle size/nm (± 1)							Extent of faceting (%)
	2	4	6	8	10	12	14	
Series 1			9	22	14	12	43	45
Series 2			12	23	16	13	36	15
Series 3	4	22	21	17	15	8	13	40

2.3 Cyclic Voltammetry

The electrochemical cell used to investigate catalyst surface morphology has been described [22] The working electrode was a Pt mesh basket containing 2–3 mg catalyst, the electrolyte was 0.5 M sulphuric acid, and potential was swept at 10 mV s^{-1} (Series 1 and 2) or 50 mV s^{-1} (Series 3). Cyclic voltammograms (CVs) showed electrosorption peaks at 0.06, 0.20, 0.28, and 0.47 V attributed (by comparison with single crystal data [14]) to the presence of $\{111\}_{terr} \times \{111\}_{step}$ step sites, $\{100\}_{terr} \times \{111\}_{step}$ step sites, {100} terraces, and {111} terraces, respectively.

The area under the voltammogram was reduced when S was adsorbed onto Pt/graphite. The surface coverage of S was calculated using the equation $\theta_s = [(Q_H{}^O) - (Q_H{}^s)]/Q_H{}^O$ where $Q_H{}^O$ and $Q_H{}^s$ are the hydrogen sorption charges before and after the sorption of S onto the Pt/graphite.

2.4 Reaction Conditions and Analysis

Reactions were conducted at 30 bar in a constant-pressure stirred reactor at ambient temperature [15]. Catalysts were rendered enantioselective by in situ modification with cinchonidine. For reactions over Series 1 and 2 catalysts, 65 mmol (7.2 ml) ethyl pyruvate, 0.17 mmol (50 mg) cinchonidine, 0.25 g catalyst and 12.5 ml dichloromethane solvent were added to the reactor in that order. The reactor was purged several times with hydrogen at 4 bar and then pressurised to 30 bar. The same procedure was adopted for Series 3 catalysts except that the quantities of ethyl pyruvate and of cinchonidine were 20 mmol and 20 mg respectively. Reaction commenced on stirring (1000 rpm); a mild initial acceleration was followed by a period of fast constant rate from which the quoted rate measurements were obtained. Analysis at 90–100% conversion was carried out by chiral gas–liquid chromatography, the products being *R*- and *S*-ethyl lactate together with a small yield of a pyruvate-lactate product [15]. All reactions favoured the formation of *R*-product.

3 Results and Discussion

3.1 Pt Particle Size Distributions

As-received Pt/graphite contained small Pt particles coalesced into clusters with an appreciable amount of connective necking [23] which disappeared on heating to 600 K (Series 1 and 3), or 700 K (Series 2). TEM images for Series 3 Pt/G catalysts have not as yet been published and are shown in Fig. 1.

Particle size distributions for catalysts sintered at 700 K are shown in Table 1. Series 1 and 2 catalysts each showed a maximum in the distribution at 8 nm, whereas Series 3 catalysts showed a maximum at 4–6 nm. The maximum in each size distribution moved to successively higher values

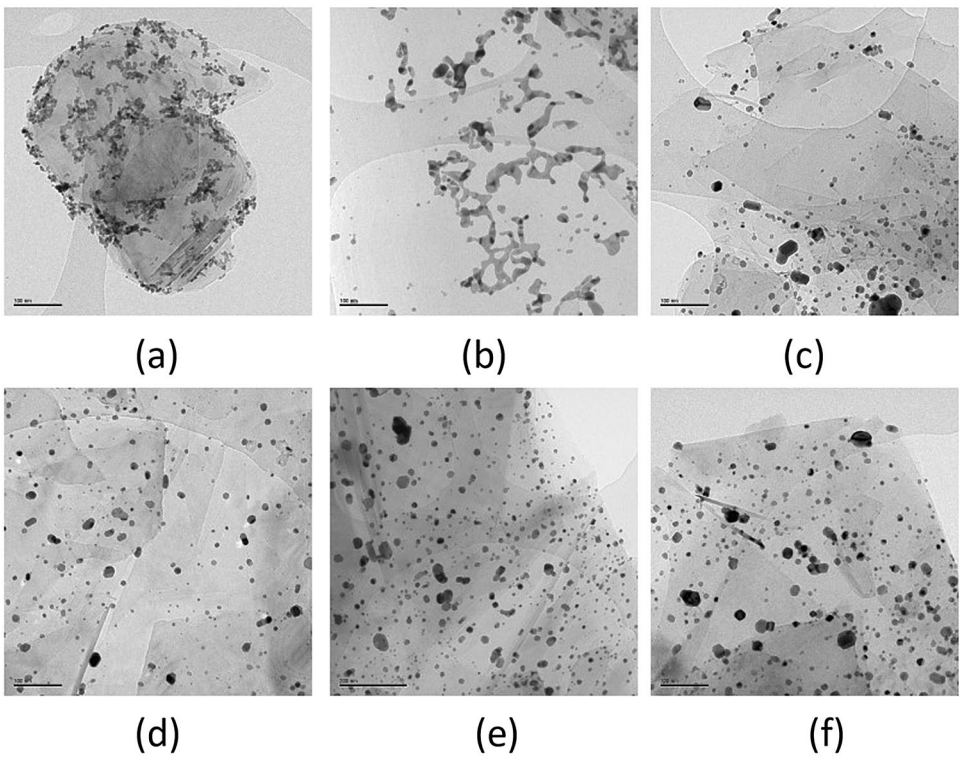

Fig. 1 TEM images of Series 3 catalysts: **a** as received and sintered in 5% hydrogen/95% argon gas mixture at **b** 450 K, **c** 600 K, **d** 700 K, **e** 800 K and **f** 900 K. The small bar in the bottom left-hand corner of each image represents 100 nm except in **e** where it represents 200 nm

at 800, 900, and 1000 K. The fractions in the 14–30 nm range varied in the sequence Series 1 > Series 2 > Series 3 (Table 1). All sintered Series 3 catalysts showed somewhat similar Pt particle size distributions, each with a maximum at 4–6 nm and with particles larger than 30 nm accounting for 20% or less of the total.

The Series 2 catalyst sintered at 1000 K in Ar showed a broad distribution as expected, with the majority of particles in the range 6–16 nm. However, the Series 1 catalyst sintered at 1000 K in H_2/Ar contained very large Pt particles, the maximum in the particle size distribution being at 30 nm, Micrographs showed 'tracks' in the graphite [23], indicating mobility of the Pt particles. This suggested that Pt-catalysed methanation may have occurred at the metal-support interface, reducing the metal-support interaction and permitting sintering by Pt particle mobility.

3.2 Faceted Particles

Pt particle growth during sintering was accompanied by faceting, i.e. the appearance of particles showing clear 120° angles. For present purposes, particles showing two or more such angular features were classed as 'faceted'. Table 1 shows values for the fraction of particles showing facets for catalysts sintered at 700 K. In general, the extent of faceting was (i) low for Series 2 catalysts, (ii) medium for all Series 3 catalysts and for Series 1 catalysts sintered at 900 K and below, and (iii) high (> 95%) for the Series 1 catalyst sintered at 1000 K.

As would be expected for sintering by atom-by-atom migration, the fraction of faceted particles increased with increasing Pt particle size. For Series 3 catalysts sintered at 700 K, particles in the 2 and 4 nm bands showed no facets; of those in the 6 and 8 nm bands 20% were faceted, in the 10–14 nm bands 70% were faceted, and 95% of particles larger than 16 nm were faceted.

3.3 Pt Surface Areas

Relative Pt surface areas were obtained from cyclic voltammetry by measurement of the H_{UPD} charge (the sum of the areas under the hydrogen underpotential deposition (Hupd) peaks) for a fixed mass of each catalyst. The measurement for the as-received material was given the value of 100 and the values for the sintered samples were scaled accordingly (Table 2). Samples sintered in the range 400–600 K in H_2/Ar lost area more rapidly than those sintered in pure Ar. However, by 800 K the relative Pt areas were comparable. The low value for the Series 1 catalyst sintered in H_2/Ar at 1000 K is consistent with its particularly large Pt particle size described above.

3.4 Voltammetric Analysis of Pt Surface Area and Enantioselective Reaction rate

Figure 2 shows the variation of platinum surface area and enantioselective reaction rate with sintering temperature for the Series 3 catalysts. Clearly, the main driver of enantioselective reaction rate is the relative amount of Pt sites available for reaction and as this varies, reaction rate changes in direct response.

3.5 Voltammetric Analysis of Pt Adsorption Sites and Enantioselectivity

Figure 3 shows a typical CV for Series 3 catalysts annealed at 700 K in H_2/Ar. Quantitative analysis of the relative populations of Pt{111} sites was undertaken in accordance with the procedures outlined in ref 24. Taking the Pt{111} anion adsorption peak at 0.4 V, the electrosorption charge was measured and used to evaluate the proportion of Pt{111} sites. [Bismuth adsorption was also used to provide a comparison [24] and excellent agreement was obtained].

Values of percentage Pt{111} character for all catalysts are listed in Table 3.

Table 3 shows that the percentage of Pt{111} character for each catalyst is strongly dependent on the sintering temperature and on the atmosphere in which sintering was conducted. For both Series 1 and Series 3 catalysts, sintering in H_2/Ar at 700 K produced a maximum in the number of Pt{111} sites formed. For Ar-sintered samples (Series 2) a gradual diminution of Pt{111} character was observed as a function of increasing sintering temperature. Other investigators have reported a correlation between enantiomeric excess and the percentage of Pt{111} terrace sites available ([17] and [20]). Results for Series 1, 2, and 3 catalysts are shown in Figs. 4, 5, and 6.

In Figs. 4 and 5 the correlation of ee with number of Pt{111} sites is confirmed. For Series 1 samples (sintered in H_2/Ar) the maximum in ee matches that for the maximum Pt{111} terrace character. In contrast, for Series 2 samples (sIntered in pure Ar), a steadily decreasing value of ee was

Table 2 Relative Pt surface areas of as-received and sintered catalysts, measured by cyclic voltammetry

Catalyst	Not sintered	400 K	450 K	500 K	600 K	700 K	800 K	900 K	1000 K
Series 1	100	59		35	34	29	24		10
Series 2	100	76		65	52	27	20		19
Series 3	100		51		45	36	25	24	

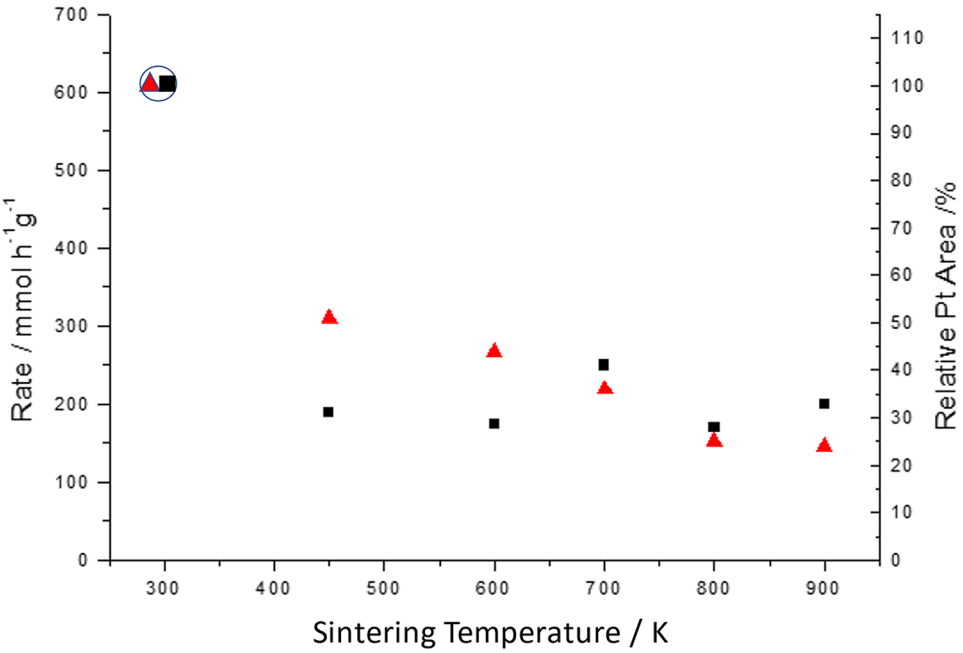

Fig. 2 Ethyl pyruvate hydrogenation over cinchonidine-modified Pt/graphite (Series 3) The effect of sintering temperature on reaction rate (left ordinate, filled squares) and on the relative Pt surface area (right ordinate, filled triangles). 293 K data points placed side by side in blue circle.

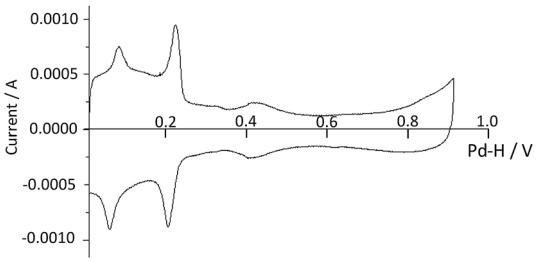

Fig. 3 CV of 5%Pt/graphite catalyst sintered in 5% hydrogen/argon at 700 K. Electrolyte was 0.5 M aqueous sulfuric acid and the sweep rate was 50 mV s^{-1}

observed as the proportion of Pt{111} adsorption sites decreased. Given the extremely low percentage of Pt{111} sites in the Series 2 catalysts a value of approximately 34% ee corresponds to the contribution of all sites other than Pt{111} to the overall value of ee under our experimental conditions (30 bar H_2 pressure/dichloromethane solvent).

For series 3 catalysts (Fig. 6) the matching-trends of ee and percentage Pt{111} character with sintering temperature was generally observed but the significant dip in ee for the catalyst sintered at 450 K is not accompanied by a reduced presence of Pt{111} surface. Rather, the CV showed that Pt{100} terrace formation was strongly enhanced, indicating that the presence of Pt{100} terraces may be reducing the overall value of ee. This hypothesis was supported when a Series 3 catalyst sintered at 500 K showed a somewhat stronger intensity of Pt{100} terrace sites and a slightly lower enantiomeric excess (see Table 4; Fig. 7).

In Table 4, the influence of sulfur adsorption on both reaction rate and ee for two catalysts sintered in 5%H_2/Ar at 500 K and 700 K are shown. Sulfur adsorption resulted in a marked decrease in reaction rate as has been reported previously [15]. However, the effect on ee of depositing sulfur is quite different for the 500 K and the 700 K sintered catalysts. For the former, selective blocking of Pt{100} sites resulted in a significant increase in ee whereas for the latter random occupation of all sites the opposite effect was observed. Thus, reductions in the Pt{100} site population (Fig. 7) caused an increase in enantioelectivity whereas a reduction in the Pt{111} site population (along with all other types of site—Fig. 8) resulted in a decrease in enantioslectivity. This concurs with a previous report, based on the behaviour of shaped nanoparticles [17], that Pt{100} terraces afford inferior ee compared to Pt{111}.

Table 3 Relative Pt{111} surface areas (%) for as-received and sintered catalysts as measured by cyclic voltammetry

Catalyst	Not sintered	Sintering temperature (K)							
		400	450	500	600	700	800	900	1000
Series 1	3.3	6.3		5.8	6.4	8.5	5.0		4.5
Series 2	3.3	2.8		2.5	3.0	2.5	2.6		2.4
Series 3	6.8		13.5		26.5	31.2	31.2	29.5	

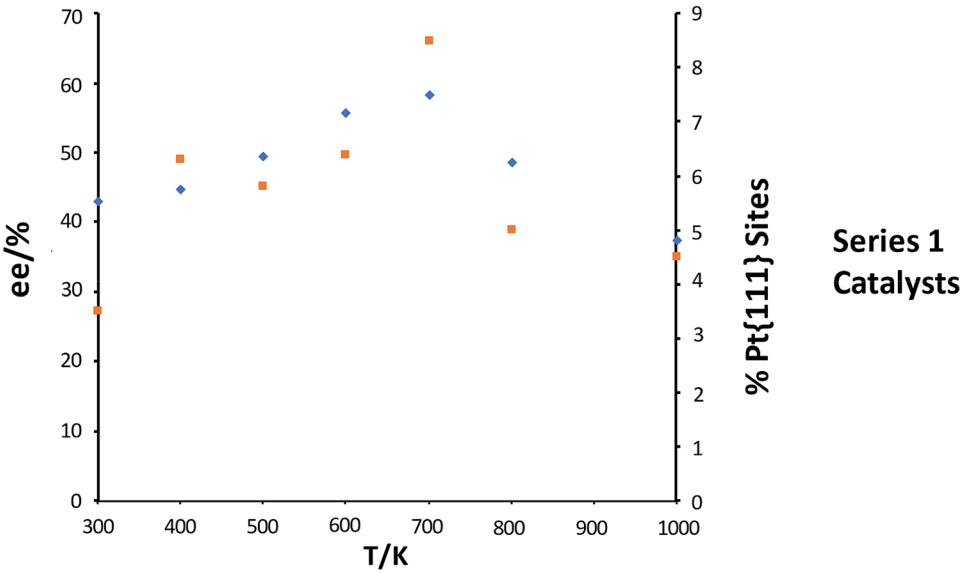

Fig. 4 Correlation between percentage Pt{111} surface sites (squares) and ee (diamonds) for Series 1 catalysts

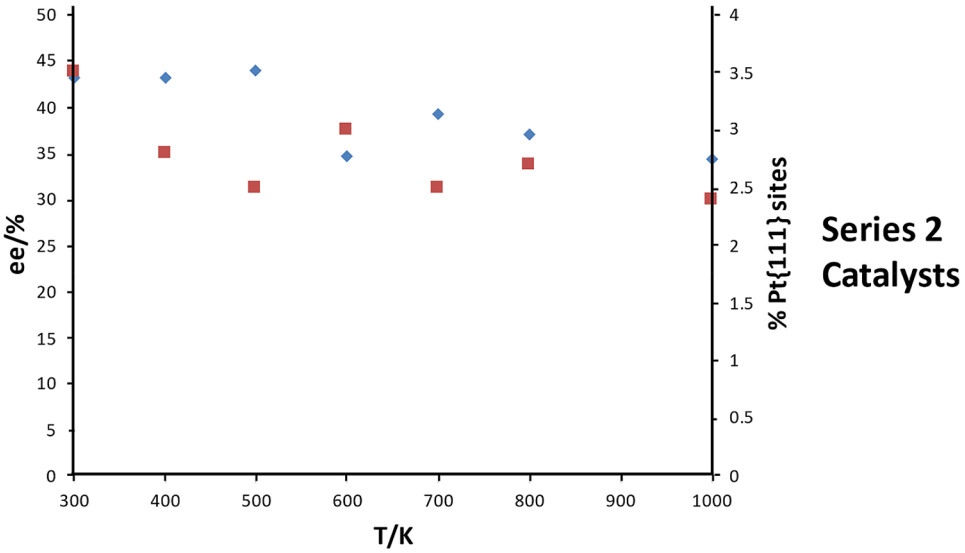

Fig. 5 Correlation between percentage Pt{111} surface sites (squares) and ee (diamonds) for Series 2 catalysts

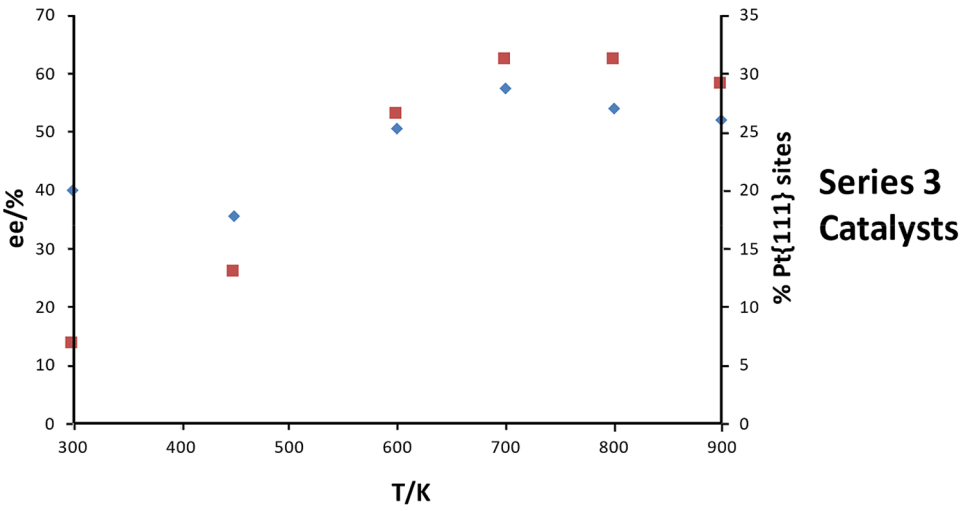

Fig. 6 Correlation between percentage Pt{111} surface sites (squares) and ee (diamonds) for Series 3 catalysts

Table 4 Variation of rate and enantioselectivity with sintering temperature for sulfur adsorption onto Pt/graphite (Series 3)

Dosing volume/cm^3	Sintering temperature (K)							
	500				700			
	0.0	0.1	0.2	0.3	0.0	0.1	0.2	0.3
Fraction of Pt surface covered by S	0.00	0.21	0.35	0.32	0.00	0.04	0.20	0.42
Reaction rate/mmol h^{-1} g^{-1}	161	65	52	52	250	79	57	20
Enantiomeric excess/%(*R*)	34.3	42.5	42.5	43.0	57.3	47.6	43.9	37.6

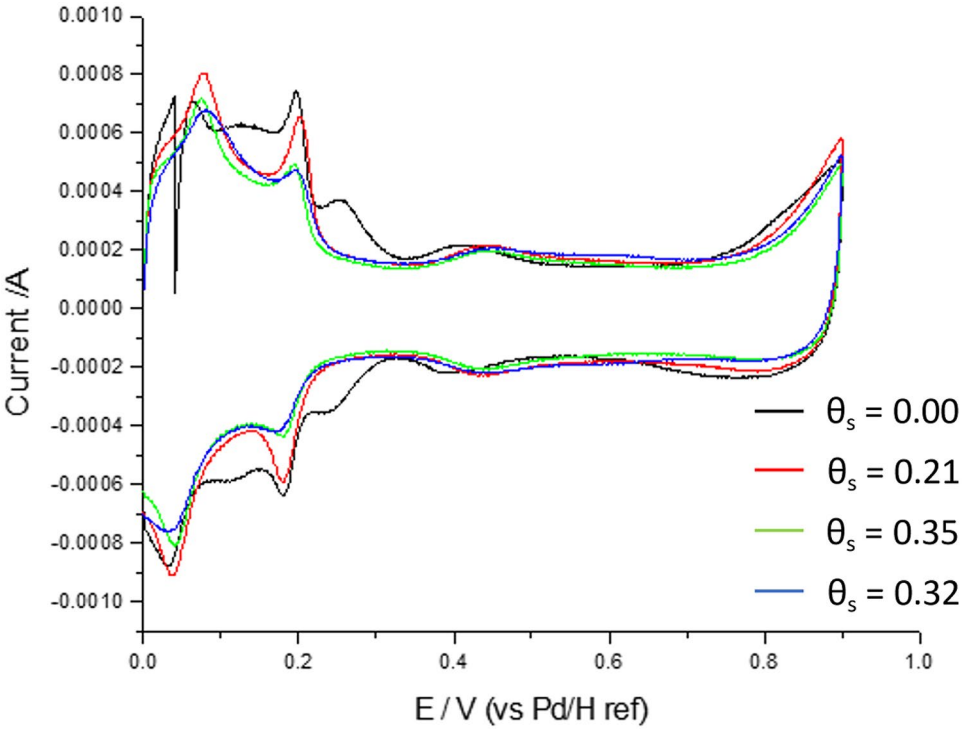

Fig. 7 The effect of S adsorption on Series 3 Pt/graphite sintered at 500 K. The Pt{100} terrace electrosorption peak is situated at 0.25 V. Sweep rate = 50 mV s^{-1}

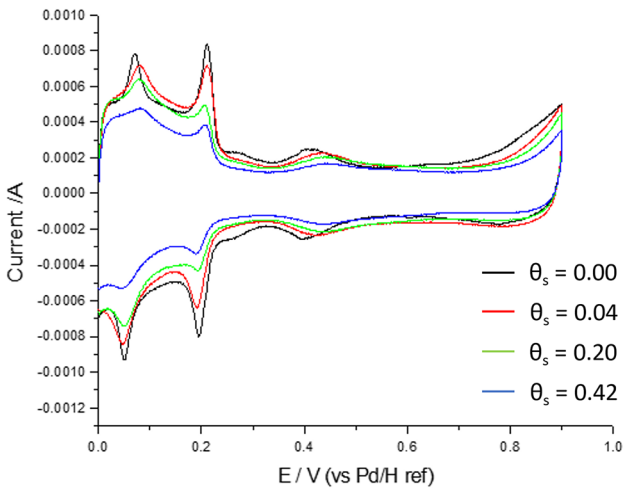

Fig. 8 The effect of S adsorption on Series 3 Pt/graphite sintered at 700 K. Sweep rate = 50 mV s^{-1}

This study presents correlations between ee and Pt{111} site availability on Series 1 and 3 catalysts (Figs. 4, 5, 6). However, Table 3 shows that Pt{111} sites are far more abundant at Series 3 surfaces than at Series 1 surfaces so —why are the values of enantiomeric excess for both Series so similar? The difference cannot be accounted for by the small differences in experimental conditions (see Experimental). We speculate that, on the surfaces of the Series 1 and Series 3 catalysts the Pt{111} terraces themselves may differ as to their nature. It has been reported previously that platinum particle size plays a crucial role in governing the overall ee attainable [25]. In order to facilitate enantioselection, a one-to-one complex between cinchonidine and ethyl pyruvate must be formed and if Pt{111} terraces are not extensive enough to accommodate the 1:1 modifier-reactant complex, then enantioselectivity may be compromised. We tentatively conclude that, although Series 3 catalysts provide

the largest proportion of Pt{111} sites, not all are functional for enantioselection.

Table 1 shows that only Series 3 catalysts contain small Pt nanoparticles (< 4 nm). Indeed, sintering produced much less particle growth in Series 3 catalysts than in Series 1 samples (see Fig. 1 and [23]). We conclude that these smaller Pt nanoparticles probably contained relatively narrow Pt{111} terraces, incapable of sustaining enantioselection. Thus, although the absolute number of Pt{111} surface atoms constituted a greater proportion of the total number of Pt surface sites in Series 3 catalysts, their functionality as sites of high ee was compromised due to their narrow average width. We propose that this hypothesis could be tested indirectly so long as one could employ a catalytic reaction that was highly sensitive to the relative number of Pt{111} surface sites but NOT the average Pt{111} terrace width. Alkyne semi-hydrogenation, as reported in reference 21 would provide such a test since the selectivity towards alkyne to alkene hydrogenation is strongly dependent on the proportion of Pt{111} sites relative to defects. Since, Series 3 catalysts exhibit a much greater proportion of Pt{111} terraces relative to Series 1 catalysts, it is predicted that the selectivity towards alkene versus alkane formation would be more pronounced. It has also been demonstrated that CO electrooxidation from Pt is highly sensitive to both particle size [26] and Pt{111} terrace width [27].In this way, a combination of alkyne hydrogenation and electrochemical stripping experiments should confirm the central hypothesis of the present study that Pt{111} average terrace width plays a crucial role in facilitating formation of the CD-EP 1:1 surface complex.

Finally, it is worth addressing the dilemma presented in the introduction as to why PVP and bismuth blocking of the same defect sites affords markedly different trends in ee [15, 20]. We note that in terms of electronic perturbation of Pt and in the absence of adsorption at Pt{111} sites, bismuth (electropositive) and sulfur (electronegative) engender opposing influences on overall ee (see [15] and Table 4, 500 K catalyst entry). Although in the present study we ascribe the blocking of Pt{100} sites as being responsible for this trend, we do not discount entirely an electronic effect of sulfur, and indeed, in the light of our experimental findings and others [17, 20] that this may also be a factor in previous bismuth adsorption studies [15]. PVP on Pt has been found, using XPS studies, to exhibit a mode of surface bonding involving the carbonyl group [28]. In Ref. [28] it was demonstrated that the direction of the charge transfer of the carbonyl-platinum bond was dependent on the size of the nanoparticle. C=O → Pt charge transfer was seen at small nanoparticle sizes (7 nm or less) and C=O ← Pt at larger sizes (> 25 nm) [28]. Hence, based on the average particle size used in reference 20, PVP is predicted to be a net electron donor to platinum. However, we also note that in reference 20 that the enhancement in ee brought about by PVP deposition only occurred after a thermal annealing step at 623 K to remove excess PVP. At this temperature, PVP on Pt nanocubes has previously been reported to undergo significant decomposition [29]. Hence, the nature of the PVP blocking species after the PVP sintering step may not correspond precisely to the adsorbed polymer measured using XPS in reference 28. We will report the influence of other chemisorbed electropositive (relative to platinum) metals on the Orito reaction in a future publication.

4 Conclusions

Cyclic voltammetry has enabled quantitative assessments to be made of the effects on enantioselectivity of basal plane exposure in Pt catalyst particles. This study complements our previous demonstration that the highest enantioselectivity is achieved at sites adjacent to steps or edges in the Pt particle structure [15].

The abundance of Pt{111}-terraces at the surfaces of sintered Pt/graphite catalysts correlates with the enantiomeric excess observed in the title reaction, whereas an increased presence of Pt{100}-terraces reduces enantioselectivity. This positive correlation holds both for catalysts sintered in 5% H_2/Ar and for catalysts sintered in pure Ar. Sintering in the presence of hydrogen gave catalysts showing values of the enantiomeric excess and of Pt{111} abundance which each passed through a maximum at a sintering temperature of 700 K. By contrast, sintering in pure Ar gave catalysts which showed continuously declining values of both enantiomeric excess and Pt{111} abundance with increasing sintering temperature, thereby highlighting the importance of surface restructuring by hydrogen during catalyst preparation. One series of catalysts sintered in H_2/Ar showed a much greater abundance of Pt{111} terraces than the other, but similar enantioselectivity. One speculative interpretation of this unexpected result is that some Pt{111} terraces may be too small in two-dimensional extent to accommodate the 1:1 chiral-modifier:reactant complexes necessary for enantioselective reaction. Possible ways of confirming the presence, or otherwise, of such non-productive Pt{111} surface (e.g. by observing the semi-hydrogenation of alkynes or by CO-stripping) are being considered. As sintering temperature was increased so the proportion of faceted Pt particles increased. The presence of facets had no significant effect on enantioselectivity (as might have been expected [16]) and did not influence the correlations of enantiomeric excess with Pt{111} abundance.

There remains an intriguing question as to why Pt/graphite, and Pt/carbon catalysts generally, are less enantioselective than Pt/silica and Pt/alumina; the answer may reside in additional electronic effects of the conducting support.

Supplementary Information The online version contains supplementary material available at https://doi.org/10.1007/s11244-021-01434-z.

Acknowledgements Financial support was provided by the Saudi Arabian Government (to A.M.S.A) and by Johnson Matthey (to D.J.J.).

Declarations

Conflict of interest We declare that we have no financial and personal relationships with other people or organizations that can inappropriately influence our work. There is no professional or other personal interest of any nature or kind in any product, service or company that could be construed as influencing the position presented in the manuscript.

References

1. Orito Y, Imai S, Niwa S (1979) J ChemSocJpn 1979:1118–1120
2. Orito Y, Imai S, Niwa S (1980) J ChemSocJpn 4:670–672
3. Wells PB, Wells RPK (2000). In: Vankelecom IFJ, Jacobs PA, De Vos DE (eds) Chiral catalyst immobilization and recycling. Wiley, Weinheim, pp 123–154
4. Bond G, Wells PB (1994) J Catal 150:329–334
5. Carley AF, Rajumon MK, Roberts MW, Wells PB (1995) J ChemSoc Faraday Trans 91:2167–2172
6. Evans T, Woodhead AP, Gutierrez-Sosa A, Thornton G, Hall TJ, Davis AA, Young NA, Wells PB, Oldman RJ, Plashkevych O, Vatras O, Agren V, Carravetta V (1999) Surf Sci 436:L691–L696
7. Blaser H-U, Jalett HP, Monti DM, Baiker A (1991) Stud Surf SciCatal 67:147–155
8. Dijkstra GDH, Kellogg RM, Wynberg H, Svendsen JS, Marko I, Sharpless B (1989) J Am ChemSoc 111:8069–8076
9. Dijkstra GDH, Kellogg RM, Wynberg H (1990) J Org Chem 55:6212–6131
10. Bürgi T, Baiker A (1998) J Am ChemSoc 120:12920–12926
11. Baiker A (2000). In: Vankelecom IFJ, Jacobs PA, De Vos DE (eds) Chiral catalyst immobilization and recycling. Wiley, Weinheim, pp 155–171
12. Simons KE, Meheux PA, Griffiths SP, Sutherland IM, Johnston P, Wells PB, Carley AF, Rajumon MK, Roberts MW, Ibbotson A (1994) ReclTravChim Pay-Bas 113:465–474
13. Geus JW, Wells PB (1985) ApplCatal 18:231–242
14. Attard GA, Gillies JE, Harris CA, Jenkins DJ, Johnston P, Price MA, Watson DJ, Wells PB (2001) ApplCatal A 222:393–405
15. Jenkins DJ, Alabdulrahman AMS, Attard GA, Griffin KG, Johnston P, Wells PB (2005) J Catal 234:230–239
16. Attard GA, Griffin KG, Jenkins DJ, Johnston P, Wells PB (2006) Catal Today 114:346–352
17. Schmidt E, Vargas A, Mallat T, Baiker A (2009) J Am ChemSoc 131:12358–12367
18. Zuo X, Liu H, Liu M (1998) Tetrahedron Lett 39:1941–1944
19. Ye J-Y, Attard GA, Brew A, Zhou Z-Y, Sun S-G, Morgan DJ, Willock D (2016) J PhysChem C 120:7532–7542
20. Chung I, Song B, Kim J, Yun Y (2021) ACS Catal 11:31–42
21. Attard GA, Bennett JA, Mikheenko I, Jenkins P, Guan S, Macaskie LE, Wood J, Wain AJ (2013) Faraday Discuss 162:57–75
22. Evans RW, Attard GA (1993) J ElectroanalChem 345:337–350
23. Attard GA, Ahmadi A, Jenkins DJ, Hazzazi OA, Wells PB, Griffin KG, Johnston P, Gillies JE (2003) ChemPhysChem 4:123–130
24. Chen Q-S, Vidal-Iglesias FJ, Solla-Gullon J, Sun S-G, Feliu JM (2012) ChemSci 3:136–147
25. Wehrli JT, Baiker A, Monti DM, Blaser H-U (1989) J MolCatal 49:195–203
26. Maillard F, Eikerling M, Cherstiouk OV, Schreier S, Savinova E, Stimming U (2004) Faraday Discuss 125:357–377
27. Lebedeva NP, Koper MTM, Herrero E, Feliu JM, van Santen RA (2000) J ElectroanalChem 487:37–44
28. Qiu LM, Liu F, Zhao LZ, Yang WS, Yao JN (2006) Langmuir 22:4480–4482
29. Borodko Y, Habas SE, Koebel M, Yang P, Frei H, Somorjai GA (2006) J PhysChem B 110:23052–23059